

Observation of magnetic focusing in two-dimensional hole systems

J. J. Heremans, M. B. Santos, and M. Shayegan

Department of Electrical Engineering, Princeton University, Princeton, New Jersey 08544

(Received 29 June 1992; accepted for publication 6 August 1992)

We report the first observation of transverse magnetic hole focusing in high quality two-dimensional hole systems confined in square and triangular quantum wells grown on (311)A GaAs substrates. The results demonstrate ballistic hole transport over distances up to 11 μm and allow us to probe the constant energy contours in k -space for these two types of confinement.

Advances in crystal growth technology have yielded increasingly pure two-dimensional electron systems (2DESs) at $\text{Al}_x\text{Ga}_{1-x}\text{As}/\text{GaAs}$ heterojunctions. Application of submicron patterning techniques on these materials to obtain laterally confined structures allows the observation of ballistic electron transport. Among such effects stands transverse magnetic electron focusing, where a beam of ballistic electrons emitted from one narrow constriction (emitter) undergoes magnetic deflection to impinge on another nearby opening (collector).¹⁻⁶

The use of transverse magnetic hole focusing (TMHF) as a probe for the intricate valence band structure of two-dimensional hole systems (2DHSs) has been recently suggested.⁷ One expects both substantial nonparabolicity and, in structures lacking inversion symmetry, a lifting of the Kramers degeneracy to affect the focusing spectra. So far, however, ballistic hole behavior has not been reported, due to the lower quality of 2DHSs. Also, the heavier mass of holes leads to a lower Fermi energy, E_F (and hence requires lower temperatures for the measurements), and a shorter mean-free-path, intrinsically putting 2DHSs at a disadvantage compared to their electron counterparts. Recently, however, significant improvements have been achieved using the (311)A plane of GaAs as the growth platform and Si as a p -type dopant.⁸⁻¹⁰ Here we report magnetic focusing experiments in such 2DHSs, which illustrate ballistic hole transport for the first time.

The samples were grown by molecular beam epitaxy on GaAs (311)A substrates, as described elsewhere.⁸⁻¹⁰ Two types of confinement were investigated: triangular wells, where the Kramers degeneracy is lifted by the lack of inversion symmetry, and roughly inversion symmetric square wells, where this degeneracy is expected to be unchanged from its bulk value, and hence to lead only to negligible splittings.¹¹⁻¹⁴ The square well consisted of a 150 \AA wide GaAs layer, flanked on both sides by 450 \AA undoped $\text{Al}_{0.3}\text{Ga}_{0.7}\text{As}$ spacers and Si-doped layers. Such double sided doping not only preserves the inversion symmetry, but also permits us to obtain a high quality 2DHS with a large hole density.¹⁵ The triangular well was formed at a single $\text{Al}_{0.35}\text{Ga}_{0.65}\text{As}/\text{GaAs}$ interface from which the dopants were separated by a 320 \AA spacer layer. Both 2DHSs were located about 1300 \AA below the surface.

Heterostructures grown on (311)A GaAs surfaces exhibit substantial transport anisotropy: higher mobilities are found along the $[\bar{2}33]$ directions than along $[01\bar{1}]$.^{9,16} These mobilities μ were measured on two connected perpendicu-

lar Hall bars oriented parallel to $[\bar{2}33]$ and $[01\bar{1}]$. Along these two directions, the square well yielded mobilities of, respectively, $1.2 \times 10^6 \text{ cm}^2/\text{V s}$ (the highest 2DHS mobility reported to date) and $4.6 \times 10^5 \text{ cm}^2/\text{V s}$ at a density $p = 3.3 \times 10^{11} \text{ cm}^{-2}$. In the triangular well, we measured $\mu = 8.2 \times 10^5 \text{ cm}^2/\text{V s}$ and $\mu = 2.5 \times 10^5 \text{ cm}^2/\text{V s}$ at $p = 1.8 \times 10^{11} \text{ cm}^{-2}$.

Wet etching, using PMMA as an etching mask after electron beam lithography, defined the TMHF patterns on a standard Hall bar. As shown in Fig. 1, barriers were oriented along both $[\bar{2}33]$ and $[01\bar{1}]$ directions. Distances between injector and collector constrictions L were 3 and 4 μm . The etchant, a dilute $\text{H}_2\text{SO}_4:\text{H}_2\text{O}_2:\text{H}_2\text{O}$ mesa etch, produced a beveled side wall for features parallel to $[01\bar{1}]$. This may somewhat obscure the conclusions that can be drawn from the difference in focusing behavior in the two perpendicular directions; let us note, however, that the etch was shallow (typically $< 1000 \text{ \AA}$) and did not reach the 2DHS. After etching, a Cr/Au front gate was deposited over the whole sample. This technique, when applied to 2DESs, resulted in focusing spectra of up to 8 periods, attesting to the damage-free patterns it produces. More particularly, this indicates that the focusing barrier possesses near total reflectivity for the carriers. Nihey *et al.* reached similar conclusions.⁵

The focusing spectra were recorded by a 4-terminal low frequency ac measurement at 0.45 K. In contrast to the electron case, no focusing could be observed at $T > 4$ K. This we ascribe to the increased thermal spread in the wave vector; denoting by k_F the Fermi wave vector and by Δk the thermal spread, we have: $\Delta k/k_F \propto m^*(k_B T)$. While at $T = 4$ K and at relevant carrier densities of $4.0 \times 10^{11} \text{ cm}^{-2}$, Δk is about 1% of k_F for electrons, it is 9% for holes (assuming an effective mass $m^* = 0.5 m_0$ for holes).

The lower panel of Fig. 2 shows square well 2DHS focusing traces at $T = 0.45$ K for different L ($L = 7 \mu\text{m}$ was obtained by combining the 3 and 4 μm distances). As expected, only one polarity of B (arbitrarily denoted by $B > 0$) yields a focusing signal. After an initial drop in collector voltage, sometimes to negative values, one or more focusing peaks develop up to $B \approx 0.15$ T on a positive slope; this slope was observed in all samples. Shubnikov-de Haas (SDH) oscillations, periodic in $1/B$, set in at higher B . For $B < 0$, the signal remains quite flat, until SDH oscillations appear again. A trace from a 2DES sample fabricated by the same method is shown in the top panel for comparison. In this case, the focusing occurs at $B < 0$.

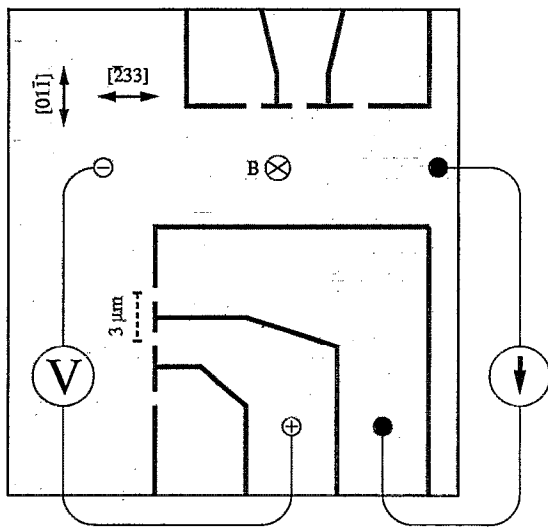


FIG. 1. Schematic of the TMHF pattern; thick black lines represent the wet etched regions. As an example, the probe configuration for a focusing distance $L=3\ \mu\text{m}$ in the $[01\bar{1}]$ direction is shown. A total of 6 different combinations can be achieved: $L=3, 4,$ and $7\ \mu\text{m}$ in two crystallographic directions.

The lithographic width W of the injector and collector constrictions in our sample was $1\ \mu\text{m}$, too large to qualify these as point contacts, even after accounting for the side wall depletion layer. As a result, interference phenomena as observed by van Houten *et al.*¹ are absent. The relatively large W/L also accounts for the fact that few focusing

peaks appear: once the cyclotron orbit fits into W , the focusing effect vanishes.

In a semiclassical approximation, valid for weak magnetic fields, the first peak in the focusing spectrum corresponds to a B where the cyclotron orbit diameter D_c is equal to L . Subsequent peaks appear at fields where L/D_c equals integer numbers, resulting in a signal periodic in B with period $B_f = (2\hbar/e)(k_F/L)$. For nonparabolic and anisotropic bands this expression retains its validity if k_F denotes the Fermi surface k -vector in the direction perpendicular to the focusing barrier.

The front gate on our sample allowed us to change the density and hence the position of the Fermi level. Using the B -field at the first peak to obtain k_F , we found that in the range of densities investigated, from 3.3×10^{11} to $4.5 \times 10^{11}\ \text{cm}^{-2}$, and to within the 5% accuracy of our data, the measured B_f are the same for both $[\bar{2}33]$ and $[01\bar{1}]$ directions and correspond to the k_F value calculated from p assuming an isotropic dispersion, i.e., from $k_F = (2\pi p)^{1/2}$. The density p was obtained from standard magnetotransport measurements performed on a Hall bar in the $[\bar{2}33]$ direction, located under the same front gate. A comparison of the SDH data at low and high fields in this Hall bar tells us that the Kramers degeneracy is not resolved at low B , as expected for an inversion symmetric square well.¹² Thus, from the TMHF and SDH data, we conclude that the square well has close to circular constant energy cross sections, resembling the free hole case. Such isotropic dispersion implies that the mobility anisotropy cannot result from band structure effects; it has indeed been suggested that its origin lies in growth induced corrugations with channels along the $[\bar{2}33]$ direction.¹⁶

Our observation of a circular Fermi surface cross section is not consistent with the band structure anisotropy expected from calculations for 2DHSs in the GaAs $\{100\}$ planes.^{7,13,14} According to these calculations, anisotropy should become noticeable for a $150\ \text{\AA}$ square well at about $k_F \approx 1 \times 10^6\ \text{cm}^{-1}$. At $k_F \approx 1.7 \times 10^6\ \text{cm}^{-1}$, as in our sample, the calculated dispersions indicate that the Fermi surface wave vector in the $\langle 010 \rangle$ directions is about 15% smaller than $(2\pi p)^{1/2}$ for the heavy hole band; this should be observable in our TMHF experiments. The band structure in the (311) plane, however, can be quite different from that in the $\{100\}$ planes; in fact, our preliminary calculations based on the formalism of Ref. 17 suggest that the former shows less anisotropy than the latter and that the 4-fold symmetry of the $\{100\}$ planes is approximately preserved in the (311) dispersion. This brings our experimental results in better agreement with theory.

In Fig. 3 we show a semilogarithmic plot of the amplitude (R_{max}) of the first focusing peak versus L , producing a straight fit to $R_{\text{max}} \propto e^{-L/l_d}$ over one order of magnitude. As first noted by Spector *et al.*,² the decay length, l_d obtained from such a fit can be related to a "focusing mean-free-path," $l_f = l_d \pi/2$, where the factor $\pi/2$ accounts for the orbit's semicircular shape. In this sample, at $p = 4.5 \times 10^{11}\ \text{cm}^{-2}$, we determine $l_f \approx 3\ \mu\text{m}$, approximately equal for the focusing barrier parallel to both $[\bar{2}33]$ and $[01\bar{1}]$. Thus, while the mobility along $[\bar{2}33]$ is about 2.6 times

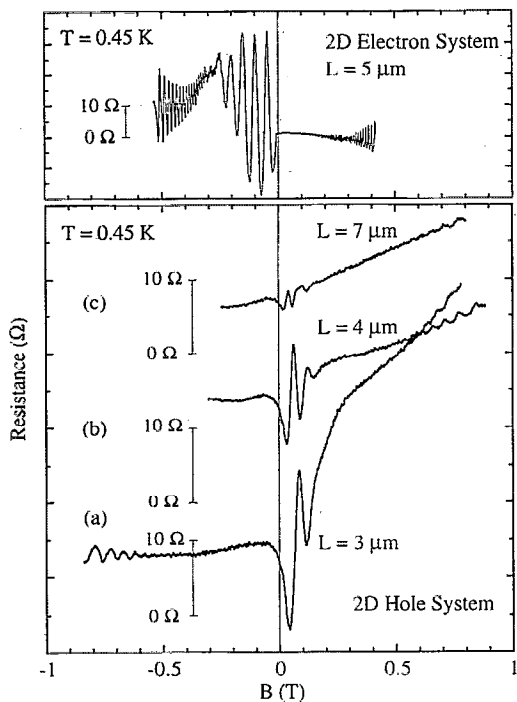


FIG. 2. Lower panel: TMHF results for the hole square well ($p=4.1 \times 10^{11}\ \text{cm}^{-2}$) with the focusing barrier along the $[01\bar{1}]$ direction. The vertical axis denotes the measured voltage at the collector divided by the injected current (scales are offset for clarity); (a) $L=3\ \mu\text{m}$; (b) $L=4\ \mu\text{m}$; (c) $L=7\ \mu\text{m}$. Upper panel: same for a conventional electron heterostructure ($n=5.9 \times 10^{11}\ \text{cm}^{-2}$) at $L=5\ \mu\text{m}$.

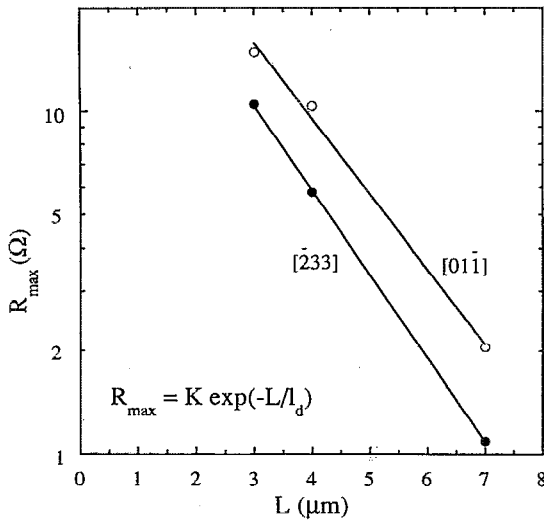


FIG. 3. Least-squares fit of the measured first peak amplitude R_{max} vs L to a form e^{-L/l_d} for TMHF spectra at $p=4.5 \times 10^{11} \text{ cm}^{-2}$ in the square well. Open circles: R_{max} measured for the barrier along $[01\bar{1}]$, $l_d=1.8 \mu\text{m}$; filled circles; barrier along $[\bar{2}33]$, $l_d=2.0 \mu\text{m}$.

larger than along $[01\bar{1}]$, l_f does not show such anisotropy. Let us also note that the ratio of the mobility mean-free-path [$l_e=(\hbar/e)\mu(2\pi p)^{1/2}$] to l_f is greater than unity. For example, in the $[\bar{2}33]$ orientation, l_e/l_f is 3.3 in this sample. This is comparable to values both Spector² and we have found for 2DESSs. These observations can be explained by the fact that different ways of averaging over scattering angles are responsible for l_f than for l_e . For instance, small angle scattering is expected to affect l_f more than l_e , leading to a ratio $l_e/l_f > 1$.²

Surprisingly, R_{max} is about twice as large with the focusing barrier along the low μ direction, $[01\bar{1}]$, than along the high μ direction, $[\bar{2}33]$. We do not yet have a clear explanation for this observation; however, it is possibly related to the etching anisotropy mentioned earlier, rather than to the hole transport anisotropy.

Finally, we also performed TMHF experiments on triangular wells with $p \approx 3.0 \times 10^{11} \text{ cm}^{-2}$ and have found k_F values again equal in both $[\bar{2}33]$ and $[01\bar{1}]$ directions but 10% larger than $k_F=(2\pi p)^{1/2}$. In addition, the SDH data show that the lack of inversion symmetry in this structure lifts the Kramers degeneracy and causes the two spin subbands to be populated unequally. From the interplay of these two spin subbands, one expects a beating in the focusing spectra; observation of such beating, however, re-

quires a large number of periods while at most two focusing peaks appear in our data. Still, comparison of these limited results with the square well data implies that the 10% discrepancy in k_F should result from the Kramers degeneracy lifting rather than from band anisotropy.

In summary, our TMHF experiments demonstrate ballistic hole transport over distances up to $11 \mu\text{m}$ ($\approx L\pi/2$ with $L=7 \mu\text{m}$). In conjunction with SDH measurements they indicate an approximately isotropic dispersion for square well confinement with p up to $4.5 \times 10^{11} \text{ cm}^{-2}$. A more complicated band structure emerges for triangular wells. Future work to probe and further elucidate the mobility and band structure anisotropy in 2DHSs is planned.

We thank K. Hirakawa, S. R. Parihar, and J. Jo for helpful discussions. This work was supported by the National Science Foundation, the Army Research Office and the Alfred P. Sloan Foundation. The authors are affiliated with the Advanced Technology Center in Photonics and Opto-Electronic Materials established at Princeton University by the State of New Jersey.

- ¹H. van Houten, C. W. J. Beenakker, J. G. Williamson, M. E. I. Broekkaart, P. H. M. van Loosdrecht, B. J. van Wees, J. E. Mooij, C. T. Foxon, and J. J. Harris, Phys. Rev. B **39**, 8556 (1989).
- ²J. Spector, H. L. Stormer, K. W. Baldwin, L. N. Pfeiffer, and K. W. West, Surf. Sci. **228**, 283 (1990).
- ³J. Spector, H. L. Stormer, K. W. Baldwin, L. N. Pfeiffer, and K. W. West, Appl. Phys. Lett. **56**, 967 (1990).
- ⁴K. Nakamura, D. C. Tsui, F. Nihey, H. Toyoshima, and T. Itoh, Appl. Phys. Lett. **56**, 385 (1990).
- ⁵F. Nihey, K. Nakamura, M. Kuzuhara, N. Samoto, and T. Itoh, Appl. Phys. Lett. **57**, 1218 (1990).
- ⁶K. Nakazato, R. I. Hornsey, R. J. Blaikie, J. R. A. Cleaver, H. Ahmed, and T. J. Thornton, Appl. Phys. Lett. **60**, 1093 (1992).
- ⁷G. Goldoni and A. Fasolino, Phys. Rev. B **44**, 8369 (1991).
- ⁸W. I. Wang, E. E. Mendez, Y. Iye, B. Lee, M. H. Kim, and G. E. Stillman, J. Appl. Phys. **60**, 1834 (1986).
- ⁹A. G. Davies, J. E. F. Frost, D. A. Ritchie, D. C. Peacock, R. Newbury, E. H. Linfield, M. Pepper, and G. A. C. Jones, J. Cryst. Growth **111**, 318 (1991).
- ¹⁰M. B. Santos, Y. W. Suen, M. Shayegan, Y. P. Li, L. W. Engel, and D. C. Tsui, Phys. Rev. Lett. **68**, 1188 (1992).
- ¹¹H. L. Stormer, Z. Schlesinger, A. Chang, D. C. Tsui, A. C. Gossard, and W. Wiegmann, Phys. Rev. Lett. **51**, 126 (1983).
- ¹²J. P. Eisenstein, H. L. Stormer, V. Narayanamurti, A. C. Gossard, and W. Wiegmann, Phys. Rev. Lett. **53**, 2579 (1984).
- ¹³D. A. Broido and L. J. Sham, Phys. Rev. B **31**, 888 (1985).
- ¹⁴M. Altarelli, U. Ekenberg, and A. Fasolino, Phys. Rev. B **32**, 5138 (1985).
- ¹⁵The relatively small valence band offset in the $\text{Al}_x\text{Ga}_{1-x}\text{As}/\text{GaAs}$ system requires the use of thin spacers to achieve a high density at single interface 2DHSs; this adversely affects the mobility.
- ¹⁶R. Noetzel, N. N. Ledentsov, L. Daeweritz, K. Ploog, and M. Hohenstein, Phys. Rev. B **45**, 3507 (1992).
- ¹⁷J.-B. Xia, Phys. Rev. B **43**, 9856 (1991).